RESEARCH ARTICLE

Target Mechanism-Based Whole-Cell Screening Identifies Bortezomib as an Inhibitor of Caseinolytic Protease in Mycobacteria

Wilfried Moreira,[a] Grace J. Y. Ngan,[a] Jian Liang Low,[a] Anders Poulsen,[c] Brian C. S. Chia,[c] Melgious J. Y. Ang,[c] Amelia Yap,[c] Justina Fulwood,[c] Umayal Lakshmanan,[c] Jolander Lim,[c] Audrey Y. T. Khoo,[c] Horst Flotow,[c] Jeffrey Hill,[c] Ravikiran M. Raju,[b] Eric J. Rubin,[b] Thomas Dick[a]

Department of Microbiology, Yong Loo Lin School of Medicine, National University Health System, National University of Singapore, Singapore[a]; Department of Immunology and Infectious Diseases, Harvard School of Public Health, Boston, Massachusetts, USA[b]; Experimental Therapeutics Center, Agency for Science, Technology and Research (A*STAR), Singapore[c]

ABSTRACT **A novel type of antibacterial screening method, a target mechanism-based whole-cell screening method, was developed to combine the advantages of target mechanism- and whole-cell-based approaches. A mycobacterial reporter strain with a synthetic phenotype for caseinolytic protease (ClpP1P2) activity was engineered, allowing the detection of inhibitors of this enzyme inside intact bacilli. A high-throughput screening method identified bortezomib, a human 26S proteasome drug, as a potent inhibitor of ClpP1P2 activity and bacterial growth. A battery of secondary assays was employed to demonstrate that bortezomib indeed exerts its antimicrobial activity via inhibition of ClpP1P2: Down- or upmodulation of the intracellular protease level resulted in hyper- or hyposensitivity of the bacteria, the drug showed specific potentiation of translation error-inducing aminoglycosides, ClpP1P2-specific substrate WhiB1 accumulated upon exposure, and growth inhibition potencies of bortezomib derivatives correlated with ClpP1P2 inhibition potencies. Furthermore, molecular modeling showed that the drug can bind to the catalytic sites of ClpP1P2. This work demonstrates the feasibility of target mechanism-based whole-cell screening, provides chemical validation of ClpP1P2 as a target, and identifies a drug in clinical use as a new lead compound for tuberculosis therapy.**

IMPORTANCE **During the last decade, antibacterial drug discovery relied on biochemical assays, rather than whole-cell approaches, to identify molecules that interact with purified target proteins derived by genomics. This approach failed to deliver antibacterial compounds with whole-cell activity, either because of cell permeability issues that medicinal chemistry cannot easily fix or because genomic data of essentiality insufficiently predicted the vulnerability of the target identified. As a consequence, the field largely moved back to a whole-cell approach whose main limitation is its black-box nature, i.e., that it requires trial-and-error chemistry because the cellular target is unknown. We developed a novel type of antibacterial screening method, target mechanism-based whole-cell screening, to combine the advantages of both approaches. We engineered a mycobacterial reporter strain with a synthetic phenotype allowing us to identify inhibitors of the caseinolytic protease (ClpP1P2) inside the cell. This approach identified bortezomib, an anticancer drug, as a specific inhibitor of ClpP1P2. We further confirmed the specific "on-target" activity of bortezomib by independent approaches including, but not limited to, genetic manipulation of the target level (over- and underexpressing strains) and by establishing a dynamic structure-activity relationship between ClpP1P2 and growth inhibition. Identifying an "on-target" compound is critical to optimize the efficacy of the compound without compromising its specificity. This work demonstrates the feasibility of target mechanism-based whole-cell screening methods, validates ClpP1P2 as a druggable target, and delivers a lead compound for tuberculosis therapy.**

Received 12 February 2015 **Accepted** 8 April 2015 **Published** 5 May 2015

Citation Moreira W, Ngan GJY, Low J. L, Poulsen A, Chia BCS, Ang MJY, Yap A, Fulwood J, Lakshmanan U, Lim J, Khoo AYT, Flotow H, Hill J, Raju RM, Rubin EJ, Dick T. 2015. Target mechanism-based whole-cell screening identifies bortezomib as an inhibitor of caseinolytic protease in mycobacteria. mBio 6(3):e00253-15. doi:10.1128/mBio.00253-15.

Editor Carol A. Nacy, Sequella, Inc.

Address correspondence to Thomas Dick, thomas_dick@nuhs.edu.sg.

With 8.6 million new cases and 1.3 million deaths annually, tuberculosis (TB), caused by *Mycobacterium tuberculosis*, remains a global infectious disease threat (1). Half a million new multidrug-resistant cases each year compound the situation. There is an urgent medical need for new drugs with new mechanism of action to control drug-resistant disease (2). After the failure of the genomics-driven, biochemical screening-based antibacterial drug discovery strategy employed during the previous decade, the field largely moved back to classical whole-cell approaches. Although empirical whole-cell strategies delivered several candidates and a new TB drug, they suffer from major drawbacks due to their "black-box" nature (3–5). The lack of target knowledge prevents the use of structure-based design during lead finding and optimization and can result in the selection of unspecific toxic compounds. Another pitfall of whole-cell-based drug discovery is that compounds might be optimized for targets that

are required only under *in vitro* culture conditions but are dispensable *in vivo* (6–8). The use of isolated biochemical targets in screening campaigns, on the other hand, often results in the identification of potent enzyme inhibitors that lack antibacterial activity because of their inability to penetrate cell membranes and accumulate within the cell (9). Engineering of compounds to penetrate bacterial cell envelopes turned out to be challenging because the physicochemical and structural rules that govern bacterial cell wall permeability are highly complex. The situation is even more challenging for mycobacteria because they have a two-membrane system: an outer membrane made up of tightly packed mycolic acids and an inner, more standard plasma membrane. The mycobacterial double-membrane system represents a formidable low-permeability barrier. This argues for a screening strategy that includes screening of targets inside the mycobacterial cell and using the double-membrane barrier as a filter. This strategy enables the selection of hits that are not only able to bind to their molecular target but also able to access it (10). Target- or pathway-based whole-cell screening methods have therefore been developed that combine the advantages of target- and cell-based approaches to identify enzyme inhibitors with antibacterial activity (11, 12). These screening methods employ pathway-selective sensitization via antisense RNA or conditional gene expression (11, 13–17) in which reduced expression of the targeted gene results in increased sensitivity to inhibitors acting on that target. Abrahams et al. used tetracycline-regulatable promoter elements to generate mycobacterial strains that conditionally express pantothenate synthetase (*panC*) and subsequently screened for compounds that display greater potency against PanC-depleted TB bacteria (13). Antisense strategies have been employed to reduce the expression of the chromosome partitioning protein ParA in *Mycobacterium smegmatis*, and compounds with antimycobacterial activity have been identified (18). Similarly, Park et al. made use of a *bioA* knockdown strain coupled with a fluorescence displacement assay to identify hits that specifically target biotin biosynthesis (19). Another type of pathway-specific strategy makes use of strains that carry a reporter gene fused to a promoter that specifically responds to certain types of disturbances, such as "cell wall synthesis stress" (20). The selective induction of the reporter signal enables screening for compounds that affect the pathway of interest. Applying this approach, Sequella, Inc., screened a library with *M. tuberculosis* carrying the RV0341 gene promoter fused to a luciferase reporter gene, identifying SQ609 (21). A similar approach has led to the identification of thiophenes as a new class of antimycobacterials that inhibit mycolic acid biosynthesis (22). Both pathway-selective sensitization and stress-induced promoter assays provide means to identify hits that are whole-cell active and pathway specific but may not provide information on the exact cellular target.

In this study, we explored the feasibility of a novel type of target-based whole-cell screening method, a target mechanism-based whole-cell approach to *Mycobacterium*. We selected the caseinolytic protease ClpP1P2 as a target, and our aim was to identify whole-cell-active inhibitors of this enzyme, thus chemically validating ClpP1P2 as a target for TB therapy and providing starting points for lead finding. Caseinolytic proteases are serine proteases found in a wide range of bacteria, including *Escherichia coli*, *Bacillus subtilis*, and *Staphylococcus aureus* (12, 23, 24). In contrast to site-specific proteases, caseinolytic proteases form a degradative complex involved in the removal of partially synthesized and misfolded proteins. In addition to these proteome housekeeping functions, caseinolytic proteases are also involved in adaptive processes by selectively removing specific regulatory functions (25). The transcription factor WhiB1 is the first protein with a regulatory function identified as being specifically degraded by mycobacterial caseinolytic protease (25). The caseinolytic protease complex is composed of catalytic protease subunits (ClpP) and regulatory subunits (ATPases). The regulatory subunits recognize substrates and provide the energy for unfolding of proteins that are to be degraded. The catalytic ClpP subunits form a degradative chamber in which proteolysis occurs. It was recently demonstrated that the proteolytic chamber of mycobacterial caseinolytic protease consists of two different subunits, ClpP1 and ClpP2, which are both essential for the growth of *M. tuberculosis* in culture and in a mouse model of TB (26, 27). Importantly, these genetic studies also suggest that the ClpP1P2 protease core represents a vulnerable target with microbicidal potential: reduced protein levels resulted in growth arrest and cell death, suggesting that a small-molecule inhibitor of ClpP1P2 should be able to inhibit proteolytic activity to a degree that causes phenotypic consequences (26). The demonstration of genetic essentiality *in vitro* and *in vivo*, vulnerability, and microbicidal potential, together with the demonstrated presence of ClpP1P2 in all clinical isolates and its—as a protease—apparent druggability, makes mycobacterial caseinolytic protease an attractive target. Furthermore, genetic ClpP1P2 depletion experiments suggest that inhibitors may show synergy with mistranslation-inducing aminoglycosides, important second-line drugs for TB, adding to the attractiveness of ClpP1P2 as a target for TB drug development.

One function of caseinolytic proteases is the removal of aborted translation products. The tmRNA trans-translation system, a bacterial rescue system that frees ribosomes stuck during protein synthesis, tags partially synthesized proteins with a caseinolytic-protease-specific (SsrA) degradation peptide (28). SsrA-tagged proteins are recognized by the caseinolytic protease and degraded. We took advantage of this mechanism and used this caseinolytic-protease-specific peptide degradation tag to develop a fluorescence-based synthetic phenotype to detect and measure intracellular ClpP1P2 inhibition. We carried out high-throughput screening (HTS), worked up the hit list with a series of secondary assays to demonstrate on-target whole-cell activity, and identified the first caseinolytic protease inhibitor with antibacterial whole-cell activity.

RESULTS

Reporter strain and assay development. Previous work has shown that the caseinolytic protease is structurally and functionally conserved in the fast-growing and nonpathogenic mycobacterial model organism *M. smegmatis* (26). We took advantage of this finding and engineered an *M. smegmatis* screening strain that allows the detection of inhibitors of intracellular ClpP1P2 activity via accumulation of SsrA-tagged green fluorescent protein (GFP). The underlying principle is that, in the undisturbed state, ClpP1P2 degrades GFP-SsrA to background fluorescence levels. An inhibitor of ClpP1P2 activity would block the degradation of tagged GFP, resulting in a gain of signal (Fig. 1A). The engineered screening strain, *M. smegmatis* pTet-GFP-SsrA, carries an episomal SsrA-tagged GFP gene placed under the control of a tetracycline-inducible promoter (Fig. 1B). A strain carrying an untagged episomal GFP gene under the control of the same tetracycline-inducible promoter (*M. smegmatis* pTet-GFP) was used as a

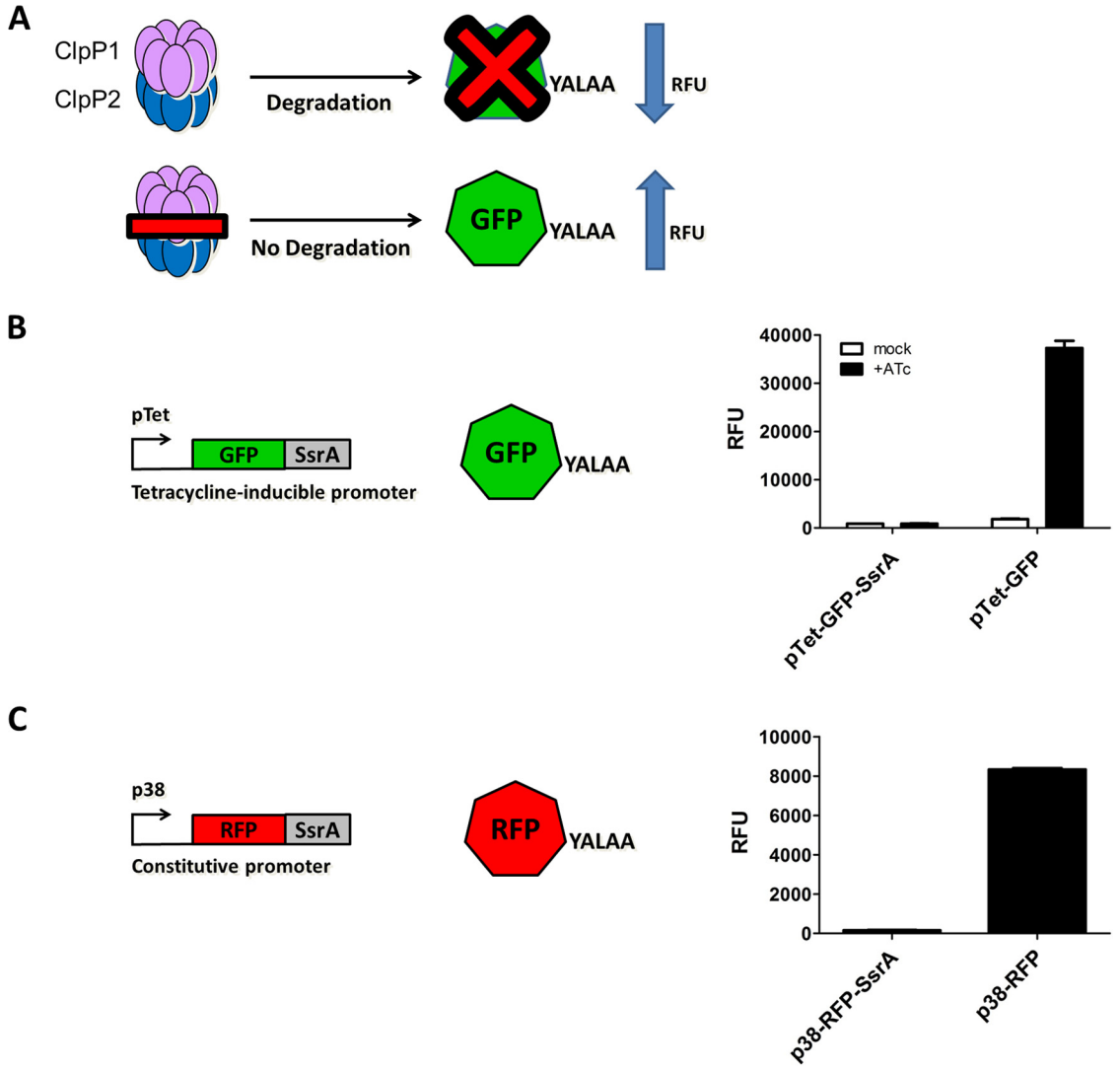

FIG 1 Reporter strains and assays. (A) Reporter assay principle. Under undisturbed conditions, ClpP1P2 protease recognizes and degrades SsrA-tagged (YALAA) GFP, resulting in a low fluorescence level. In the presence of a ClpP1P2 inhibitor, GFP is not degraded. Its accumulation results in an increase in fluorescence. (B) *M. smegmatis* pTet-GFP-SsrA/pTet-GFP and assay activities. SsrA-tagged GFP (or untagged GFP) expression has been placed under the control of an ATc-inducible promoter (pTet). In the absence of ATc induction, the fluorescence signal level remains basal with both SsrA-tagged and untagged GFP. In the presence of ATc, fluorescence is low in Smeg-pTet-GFP-SsrA because of GFP degradation, whereas fluorescence increases in cultures expressing untagged GFP. (C) *M. smegmatis* p38-mRFP-SsrA/p38-mRFP and assay activities. Similarly, SsrA-tagged RFP (or untagged RFP) expression has been placed under the control of a constitutive promoter (p38). The fluorescence signal is low in a Smeg-pTet-RFP-SsrA culture because of RFP degradation, whereas it increases in a culture expressing untagged RFP. Shown is the average of three independent experiments with error bars representing the standard deviation.

control for GFP expression and, as a small-molecule ClpP1P2 inhibitor for use as a positive control in the assay was not available, to provide an estimated upper fluorescence signal level upon complete inhibition of GFP-SsrA degradation in the screening strain (Fig. 1B).

We developed a reporter assay in a 384-well plate format for HTS. In the optimized assay format, bacteria were seeded into 30 μl at a low density (optical density at 600 nm [OD_{600}] of 0.2, log phase) and incubated for 3 h (to remain within 1 generation time) in the presence or absence of the inducer anhydrotetracycline (ATc) at 50 ng/ml prior to GFP fluorescence signal measurement. Figure 1B shows that after 3 h of induction with ATc, the screening strain *M. smegmatis* pTet-GFP-SsrA showed low-level background fluorescence, whereas high fluorescence levels were detected in the strain expressing the untagged version of GFP (*M. smegmatis* pTet-GFP). The assay was assessed by pilot screening with a small collection of 1,600 compounds (PHARMAKON) to examine its robustness and reproducibility. The corresponding performance indicators were satisfactory, with a signal-to-noise ratio of 5.6 $\pm$ 0.3, a Z′ factor of 0.8 $\pm$ 0.1, and a low hit rate of 0.5%.

HTS: 1,000 primary hits. A library of 503,879 compounds was screened at a single-point concentration of 10 μM. Performance indicators were again satisfactory with a signal-to-noise ratio of 3.8 $\pm$ 1 and a Z′ factor of 0.8 $\pm$ 0.1. With a cutoff of two times the standard deviation of the mean value of all of the compounds, 1,033 primary hits were identified (0.2% hit rate) (Fig. 2). Autofluorescent compounds were eliminated, and nonfluorescent or

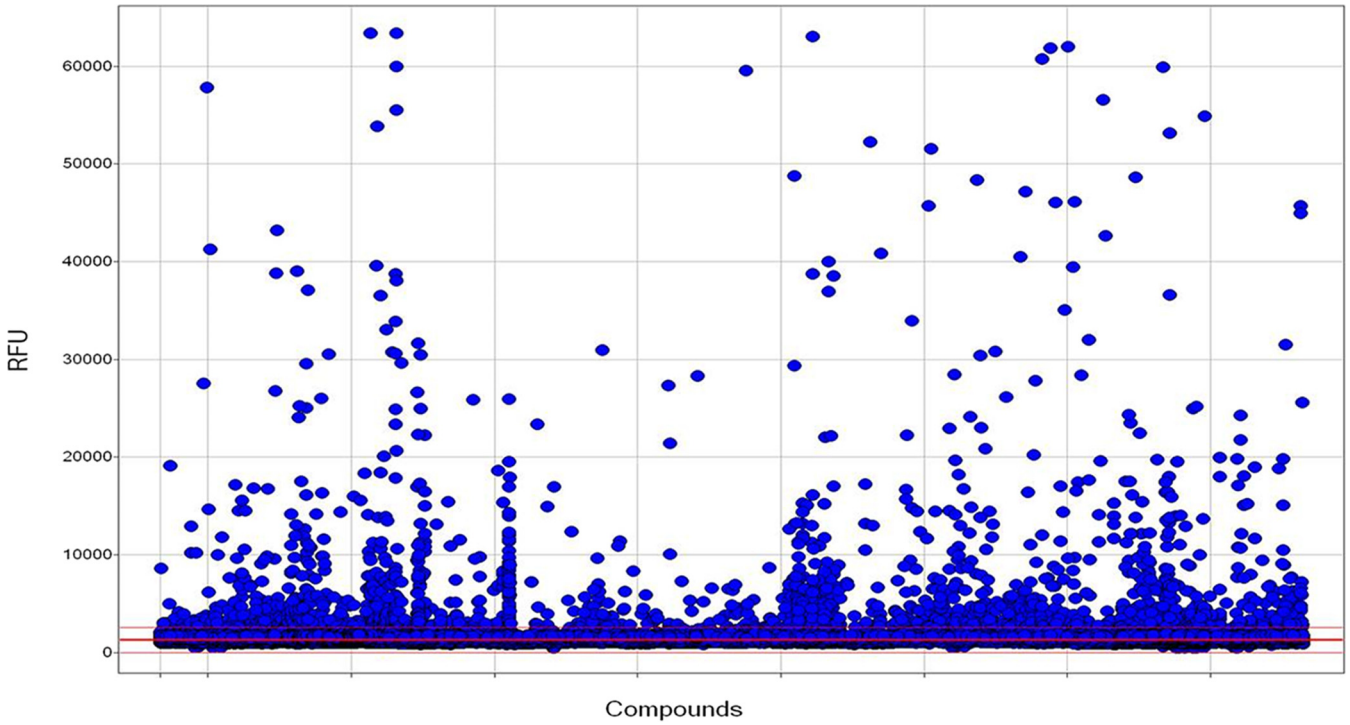

FIG 2 Scatterplot of primary hits from HTS. A library of half a million compounds was screened at a single concentration of 10 μM for inhibitors of ClpP1P2 activity in *M. smegmatis* carrying GFP-SsrA under the control of pTet (Fig. 1B). Compound mean fluorescence is represented by the red line. A threshold of two times the standard deviation of the mean (pink line) was used as the cutoff for hit selection.

low-fluorescence hits ($n = 209$) were subjected to a 10-point dose-response assay. Compounds that showed any type of dose response and were available as powders ($n = 89$) were characterized further (Fig. 3).

Secondary ClpP1P2 activity-based assay: three survivors. To exclude false-positive hits due to interference with the tetracycline-dependent pTet-GFP-SsrA reporter system of the screening strain, we employed a second reporter system for

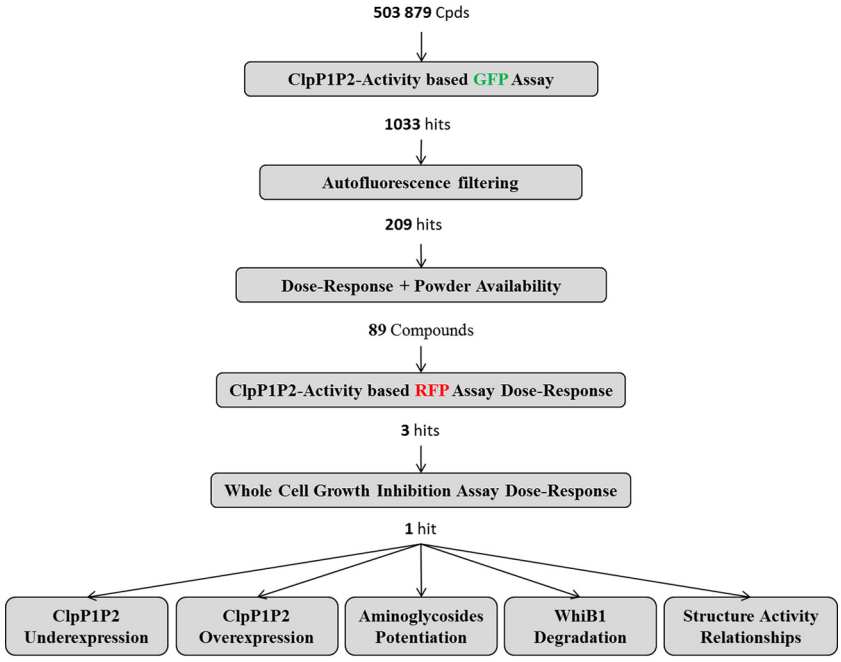

FIG 3 Screening cascade and workup of hits. See Results for details. Cpds, compounds.

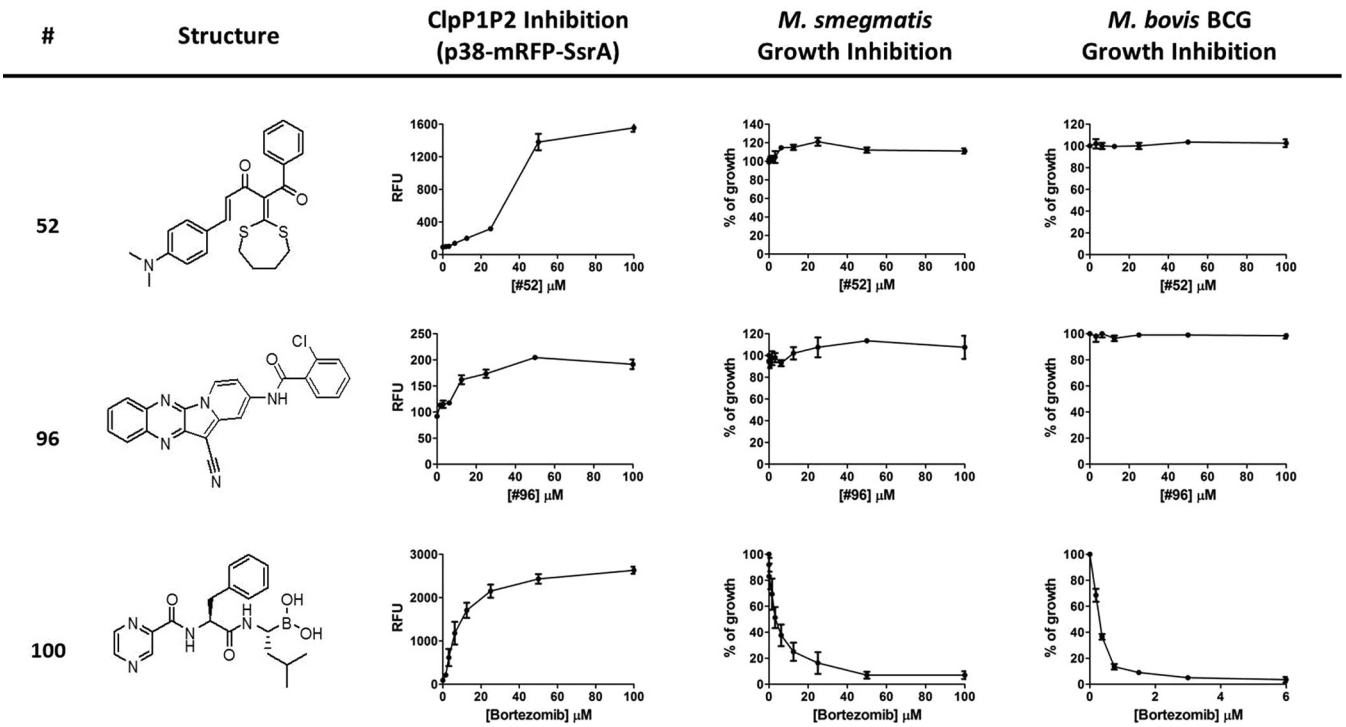

FIG 4 ClpP1P2 activity and growth inhibition of prioritized hits. Shown are the compound structures, the ClpP1P2 activity dose response in *M. smegmatis* p38-mRFP-SsrA, and the growth inhibition dose response in *M. smegmatis* and *M. bovis* BCG. The experiments were carried out three times and showed the same results. One representative example is depicted.

ClpP1P2 activity in which both the promoter and the reporter were different from the system used for primary screening: the SsrA-tagged mCherry red fluorescent protein (mRFP) gene placed under the control of a constitutive p38 promoter (*M. smegmatis* p38-mRFP-SsrA, Fig. 1C). A strain carrying an untagged version of the reporter protein (*M. smegmatis* p38-mRFP) was used again as a positive control for signal acquisition (Fig. 1C). With this assay and compound solutions newly prepared from powder stocks, three hits were selected that induced a significant and dose-dependent increase in mRFP fluorescence (compounds 52, 96, and 100, Fig. 4).

Taken together, it is notable that we observed a very low rate of hit confirmation. Of 1,033 primary single-point hits identified in the GFP readout assay, we lost 80% because of autofluorescence. Of the 209 hits with low or no fluorescence, we again lost more than 50% because of a lack of a dose response in the same assay (and powder availability). Of the 89 hits available in powder form and dose response positive, only three were confirmed in the orthogonal, mRFP readout-based dose-response assay. Fluorescence readouts are notorious for high false-positivity rates. Furthermore, screening for autofluorescence was carried out only with pure compounds, i.e., in the absence of bacteria. This may have contributed to the low confirmation rate, since the fluorescence properties of small molecules are dependent on their local, for instance, aqueous versus lipid membrane, environment.

Growth inhibition activity of potential ClpP1P2 inhibitors: one survivor. To determine whether any of the three candidate ClpP1P2 inhibitors showed antibacterial activity, we carried out eight-point growth inhibition assays with *M. smegmatis* and turbidity as a readout. Figure 4 shows that whereas compounds 52 and 96 did not display any growth inhibition activity at concentrations of up to 100 μM, compound 100 showed an MIC_{50} of 4 μM, comparable to a ClpP1P2 50% inhibitory concentration (IC_{50}) of 6 μM (Fig. 4). Determination of the microbicidal activity of compound 100 showed that its MBC_{90}, the minimum bactericidal concentration that kills 90% of an initial inoculum, was 30 μM.

The compounds were also tested for growth inhibition potency against *Mycobacterium bovis* BCG, and compound 100 again showed clear growth inhibition (MIC_{50} = 0.3 μM), whereas the other two compounds did not inhibit growth at up to 100 μM (Fig. 4). Determination of the microbicidal activity of compound 100 showed that its MBC_{90} for *M. bovis* BCG was, at 0.75 μM, also accordingly lower. We also confirmed the growth inhibition potency of compound 100 against virulent *M. tuberculosis* H37Rv (MIC_{50} = 0.8 μM). It is interesting that compound 100 was more potent against tubercle bacilli (MIC_{50} = 0.3 or 0.8 μM) than against *M. smegmatis* (MIC_{50} = 4 μM; see Discussion).

The survivor: BZ, a human proteasome inhibitor. The whole-cell-active candidate ClpP1P2 protease inhibitor compound 100 (Fig. 4) is the dipeptide-boronic acid bortezomib (BZ; Velcade, Cytomib). BZ is the first proteasome inhibitor approved by the U.S. FDA for the treatment of newly diagnosed multiple myeloma and relapsed/refractory multiple myeloma and mantle cell lymphoma (29–31). The human proteasome, like bacterial caseinolytic protease, is a degradative protease complex involved in proteome housekeeping in humans. The boronic acid warhead of BZ forms a covalent adduct to the catalytic hydroxyl group of threonine in the active site of the proteasome, resulting in enzyme dys-

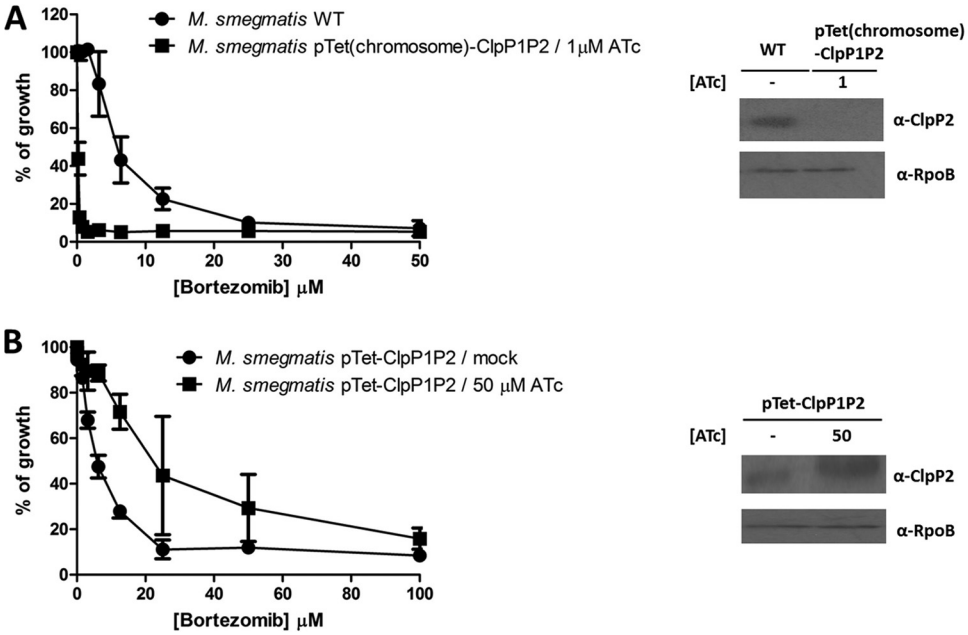

FIG 5 Growth inhibition activity of BZ in bacteria with decreased and increased ClpP1P2 levels. (A) ClpP1P2 underexpression in *M. smegmatis* pTet(chromosome)-ClpP1P2. BZ growth inhibition was assessed in an *M. smegmatis* strain in which the expression of the chromosomal ClpP1 and ClpP2 genes was placed under the control of a pTet promoter. A low ATc inducer concentration, 1 μM, resulted in a level of ClpP2 expression lower than that in a WT *M. smegmatis* culture, as confirmed by the Western blot assay on the right. On the left, the effect of a lower ClpP1P2 level on BZ susceptibility is shown. (B) ClpP1P2 overexpression in *M. smegmatis* pTet-ClpP1P2. This strain carries, in addition to a chromosomal copy, an episomal copy of ClpP1P2 placed under the control of an ATc-inducible pTet promoter. A high inducer concentration, 50 μM, resulted in a level of ClpP2 higher than that in the uninduced control, as confirmed by the Western blot assay on the right. On the left, the effect of an increased ClpP1P2 level on BZ susceptibility is shown. Anti-RpoB antibody probing was carried out to confirm equal protein loading. Shown in the growth inhibition experiment results are the averages of three independent experiments, with error bars representing the standard deviations. The Western blot assays were carried out three times and showed the same results. One representative example is shown.

function and leading to cell cycle arrest and apoptosis in cancer cells (32, 33).

Growth inhibition activity of BZ in bacteria with decreased and increased ClpP1P2 levels. The identification of the proteasome (protease) inhibitor BZ as an inhibitor in our cell-based ClpP1P2 proteolytic activity assay suggests that BZ might directly inhibit the catalytic protease subunits of the caseinolytic protease complex ClpP1P2. To determine whether the growth inhibition effect of BZ is indeed due to interference with ClpP1P2 (and not some other caseinolytic protease complex-related or -unrelated targets), we measured the effect of reducing and increasing intracellular ClpP1P2 levels on the growth inhibition activity of the compound. Reducing the level of ClpP1P2 is expected to increase the sensitivity of the bacterium to the compound, whereas increasing the level is expected to decrease the sensitivity of cells.

To generate cultures of bacteria with lower and higher ClpP1P2 levels than the wild type (WT), we employed two different *M. smegmatis* strains in which the ClpP1 and ClpP2 genes are under the control of a tetracycline-dependent promoter. To generate *M. smegmatis* with a reduced ClpP1P2 level, we employed *M. smegmatis* pTet(chromosome)-ClpP1P2, in which the expression of the native (i.e., chromosomal) ClpP1P2 genes was placed under the control of a tetracycline-dependent promoter (26). In this strain, the level of ClpP1P2 can be modulated as a function of added concentrations of the inducer ATc. The Western blot analysis in Fig. 5A shows that at a low ATc concentration (1 μM), the ClpP1P2 protease level was indeed reduced. The comparative growth inhibition experiments with a low-level ClpP1P2 culture and WT bacteria depicted in Fig. 5A show that reduction of the ClpP1P2 protein level indeed resulted in pronounced hypersensitization of the bacteria to BZ: the MIC_{50} of BZ shifted down from 4 to 0.5 μM.

To generate *M. smegmatis* with an increased ClpP1P2 level, we employed *M. smegmatis* pTet-ClpP1P2, a strain that carried, in addition to the WT chromosomal ClpP1P2-encoding genes, an episomal copy of ClpP1P2 under the control of the same tetracycline-inducible promoter mentioned above (26). Addition of ATc at an appropriate high concentration (50 μM) increased the level of ClpP1P2, as shown in the Western blot analysis in Fig. 5B. Figure 5B also shows that the increase in the ClpP1P2 level desensitized the bacteria: BZ's MIC_{50} shifted from 4 to 20 μM. Taken together, the ClpP1P2 under- and overexpression results, showing an inverse correlation between the candidate target level and antibacterial drug susceptibility, suggest that BZ inhibits whole-cell growth by targeting ClpP1P2.

In the growth inhibition experiment with WT *M. smegmatis*, only BZ/compound 100 showed an effect. Compounds 52 and 96, weakly positive in the reporter ClpP1P2 activity assays, did not show any antibacterial activity (Fig. 4). To determine whether whole-cell antibacterial activity might be detectable in sensitized bacteria with a reduced ClpP1P2 level, we determined the effectiveness of compounds 52 and 96 against underexpressing cultures of *M. smegmatis* pTet(chromosome)-ClpP1P2. However, no effect on growth was observed at concentrations of up to 100 μM

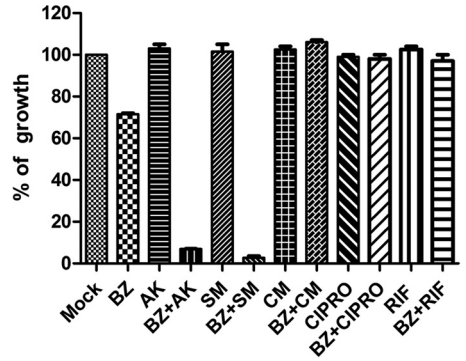

FIG 6 Combination of BZ and antibiotics. WT *M. smegmatis* was treated with subinhibitory concentrations of BZ (1.5 μM), amikacin (AK, 0.4 μM), streptomycin (SM, 0.05 μM), chloramphenicol (CM, 4.5 μM), ciprofloxacin (CIPRO, 0.09 μM), or rifampin (RIF, 0.75 μM), independently or in combination as indicated. After 24 h, growth was assessed via OD_{600} measurement. Shown is the average of three independent experiments with error bars representing the standard deviation.

(data not shown). This suggests that compounds 52 and 96 do not act via ClpP1P2. Whether these two compounds act via other, nonproteolytic components of the caseinolytic protease complex, such as the regulatory ATPases, or whether their apparent reporter activity in the ClpP1P2 fluorescence assays is an artifact remains to be determined.

Combination of BZ with aminoglycosides. Genetic depletion experiments showed previously that bacteria with a reduced ClpP1P2 level display increased sensitivity to the aminoglycosides amikacin and streptomycin, supporting the notion that mycobacterial ClpP1P2 is involved in the removal of mistranslated proteins, as shown for other bacteria (26). This potentiation effect of protein synthesis inhibitors was specific for the mistranslation-inducing aminoglycosides, whereas no potentiation was observed with the ribosome-stalling antibiotic chloramphenicol (34). If BZ is an authentic small-molecule ClpP1P2 inhibitor, the drug is expected to copy that phenotype. Figure 6 shows that the predicted selective potentiation effect can indeed be observed. A combination of subinhibitory concentrations of BZ and amikacin or streptomycin caused complete growth inhibition, whereas BZ had no potentiation effect on chloramphenicol. Taken together, the drug combination experiment results show that BZ copies the selective aminoglycoside hypersensitivity phenotype observed in ClpP1P2-underexpressing bacteria, consistent with BZ being an inhibitor of this protease.

Effect of BZ on the level of the caseinolytic protease substrate WhiB1. Genetic experiments combined with quantitative proteomic and transcriptomic analyses recently identified the first specific protein substrate of ClpP1P2, the transcription factor WhiB1. Depletion of ClpP1P2 resulted in the accumulation of this DNA binding protein (26). If BZ is an authentic ClpP1P2 inhibitor, exposure of the bacteria to the compound is expected to copy the effect of ClpP1P2 underexpression on WhiB1 and result in an increase in the WhiB1 protein level. To determine the effect of BZ on the degradation of WhiB1, we again employed an *M. smegmatis* reporter strain expressing tetracycline-inducible GFP but with WhiB1 as a ClpP1P2-specific degradation "tag" instead of the SsrA tag used for the primary screening (*M. smegmatis* pTet-GFP-WhiB1, Fig. 7A and B). Figure 7B shows that BZ exposure increased fluorescence in a dose-dependent manner, suggesting that the drug indeed inhibits the ClpP1P2-dependent degradation of WhiB1, resulting in the accumulation of GFP-WhiB1. Figure 7C shows that this effect of BZ on the GFP signal was WhiB1 dependent: BZ did not affect the fluorescence of an *M. smegmatis* culture carrying the same episomal pTet-GFP construct but with GFP lacking the WhiB1 tag. Our finding that BZ blocks the degradation of the caseinolytic protease substrate WhiB1 further supports the model in which the drug exerts its antibacterial activity via modulation of ClpP1P2.

Correlation between ClpP1P2-dependent proteolytic-activity and growth inhibition potencies of structural derivatives of BZ. Apparent dose-dependent ClpP1P2 protease inhibition in two strains carrying different ClpP1P2 activity-based SsrA reporter systems, expected susceptibility shifts in ClpP1P2-under- and -overexpressing strains, specific synergy with aminoglycosides, and accumulation of the ClpP1P2 substrate WhiB1 upon BZ exposure all support the notions that BZ inhibits ClpP1P2 and that it is via this interaction that the compound exerts its whole-cell growth-inhibitory activity.

A powerful independent method to show that a particular chemical scaffold exerts its whole-cell growth inhibition effect via modulation of a particular target is based on demonstrating a correlation between the two (whole-cell versus enzyme) structure-activity relationships. The concept is to identify structural derivatives of the scaffold that cover a range of enzyme inhibition activities (high, medium, and no potency) and determine whether the IC_{50}s for the enzyme correlate with whole-cell MIC_{50}s. A positive correlation argues for an on-target effect. Figure 8A shows three BZ derivatives CEP-18770, MNL-2238, and MG-262. CEP-18770 and MNL-2238 are second-generation proteasome inhibitors, and MG-262 is another boronate peptide showing activity against the human proteasome (35–38). Figure 8B shows that these three compounds show high (CEP-18770, same activity as BZ itself) and medium (MNL-2238, MG-262) inhibitory potencies in the cell-based fluorescence assay measuring ClpP1P2 proteolytic activity (*M. smegmatis* p38-mRFP-SsrA). Figure 8C shows that the whole-cell growth-inhibitory activities of the compounds follow the same pattern: CEP-18770 shows the same potent growth inhibition as BZ. The weaker inhibitors in the ClpP1P2 reporter assay, MNL-2238 and MG-262, also show weaker growth inhibition. The observed correlation between potency against ClpP1P2 and growth inhibition of BZ analogues suggests that the drug acts via the assumed target.

Dependence of the ClpP1P2- and growth-inhibitory activities of BZ on its boronic acid warhead. The boronic acid warhead of the human proteasome inhibitors reacts covalently with the active-site threonine hydroxyl moiety of the proteasome and is important for the selectivity and potency of the compounds. For MG-262, for instance, it has been shown that replacement of the boronic acid warhead with an aldehyde resulted in 100-fold-reduced activity against the proteasome (35, 36). Similarly, BZ was developed as a more potent analogue of its peptide aldehyde counterpart (37, 38). Assuming a similar boronic acid-dependent mechanism for the inhibition of the mycobacterial ClpP1P2 serine proteases, the prediction is that removal of the warhead results in the simultaneous loss of activity of the compound in both the cellular ClpP1P2 activity and the growth inhibition assay. Figure 8A shows the aldehyde derivatives of BZ and MG-262, BZ-al and MG-132, respectively. Figure 8B and C show that replacement

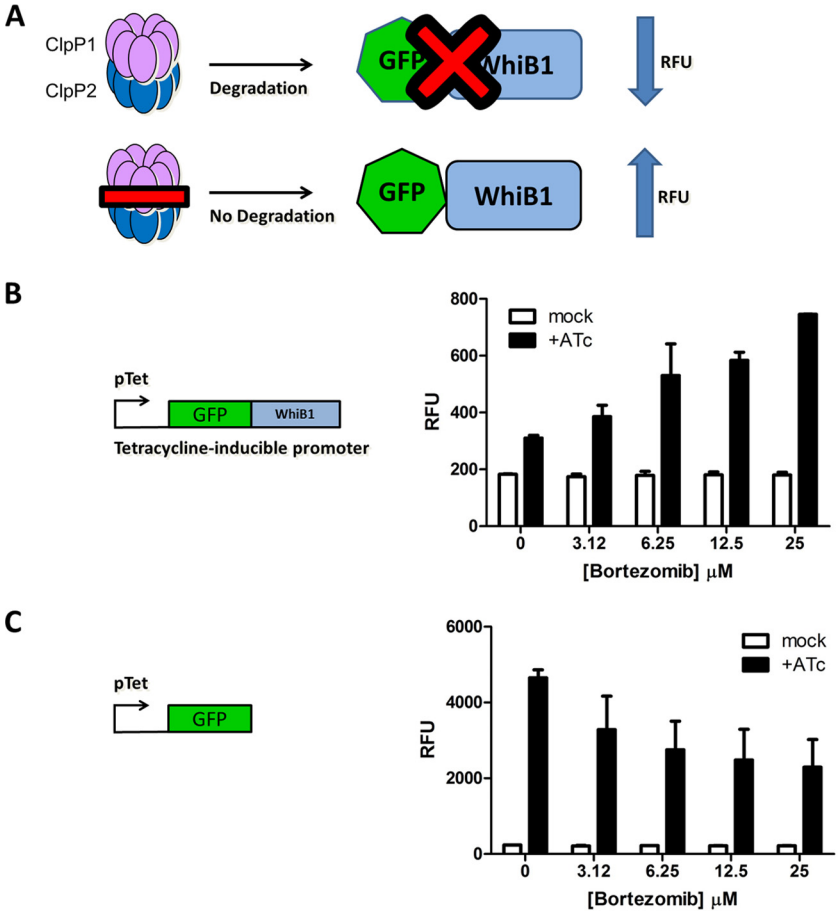

FIG 7 Effect of BZ on the level of the caseinolytic protease substrate WhiB1. (A) Reporter strain principle. WhiB1 is a substrate of ClpP1P2. Under undisturbed conditions, GFP-WhiB1 is recognized and degraded, resulting in a basal level of fluorescence. In the presence of an inhibitor of ClpP1P2, degradation is reduced and GFP-WhiB1 accumulates, resulting in an increase in fluorescence. (B) WhiB1-GFP has been placed under the control of the pTet promoter and introduced episomally into *M. smegmatis*. *M. smegmatis* pTet-GFP-WhiB1 was exposed to increasing concentrations of BZ for 6 h in the presence or absence of the inducer (ATc), upon which fluorescence was measured. (C) *M. smegmatis* pTet-GFP was used as a control, demonstrating the WhiB1 dependence of the fluorescence increase shown in panel B. Shown is the average of at three independent experiments, with error bars representing the standard deviation.

of boronic acid with aldehyde completely abrogated both the enzyme- and growth-inhibitory activities of the two compounds. These results show that the boronic acid warhead is essential for anti-ClpP1P2 proteolytic and antibacterial activities and indicate that BZ inhibits ClpP1P2 via covalent modification of its active sites.

Modeling of inhibitors with a boronic acid warhead into *M. tuberculosis* ClpP1P2. Both ClpP1 and ClpP2 are heptamers, and each has seven catalytic sites. The boronic acid-based inhibitors (Fig. 8) were modeled into the ClpP1 and ClpP2 catalytic sites and covalently attached to the serine of the catalytic triad (Ser98 and Ser110 in ClpP1 and ClpP2, respectively). All of the nitrogen and oxygen atoms of the inhibitor amide groups hydrogen bond with the protein backbone. One oxygen of the boronic acid occupies the oxyanion hole, while the other forms a salt bridge to the catalytic histidine (His123 and His135 of ClpP1 and ClpP2, respectively). This is shown in Fig. 9 for BZ modeled into one of the ClpP1 sites. The P1 site is hydrophobic in both ClpP1 and ClpP2, consistent with the hydrophobic side chain of the inhibitors. Neither ClpP1 nor ClpP2 has a proper P2 site, and the P2 side chain of the inhibitors makes poor contacts with the protein. BZ, CEP-18770, and MNL-2238 modeled well into both the ClpP1 and ClpP2 sites. MG-262 has an extra residue compared to the other inhibitors, and this compound did not model well because of the P3 side chain clashing with the protein (data not shown). This is consistent with the observed enzyme-inhibitory activities shown in Fig. 8B, in which MG-262 was the least potent compound of the four.

DISCUSSION

Here, we developed a novel type of antimycobacterial screening method by attempting to combine the advantages of target mechanism and whole-cell approaches: a target mechanism-based whole-cell screening method. The degradative caseinolytic protease ClpP1P2 was selected as a target, and a reporter strain with a synthetic phenotype was engineered that allowed the detection of inhibitors via intracellular accumulation of GFP. A 500,000-compound library was screened, and the human proteasome inhibitor BZ was found to be positive in two independent whole-cell reporter assays measuring ClpP1P2 proteolytic activity. The compound showed growth inhibition and microbicidal activity in the screening strain of *M. smegmatis* used, as well as in the tubercle

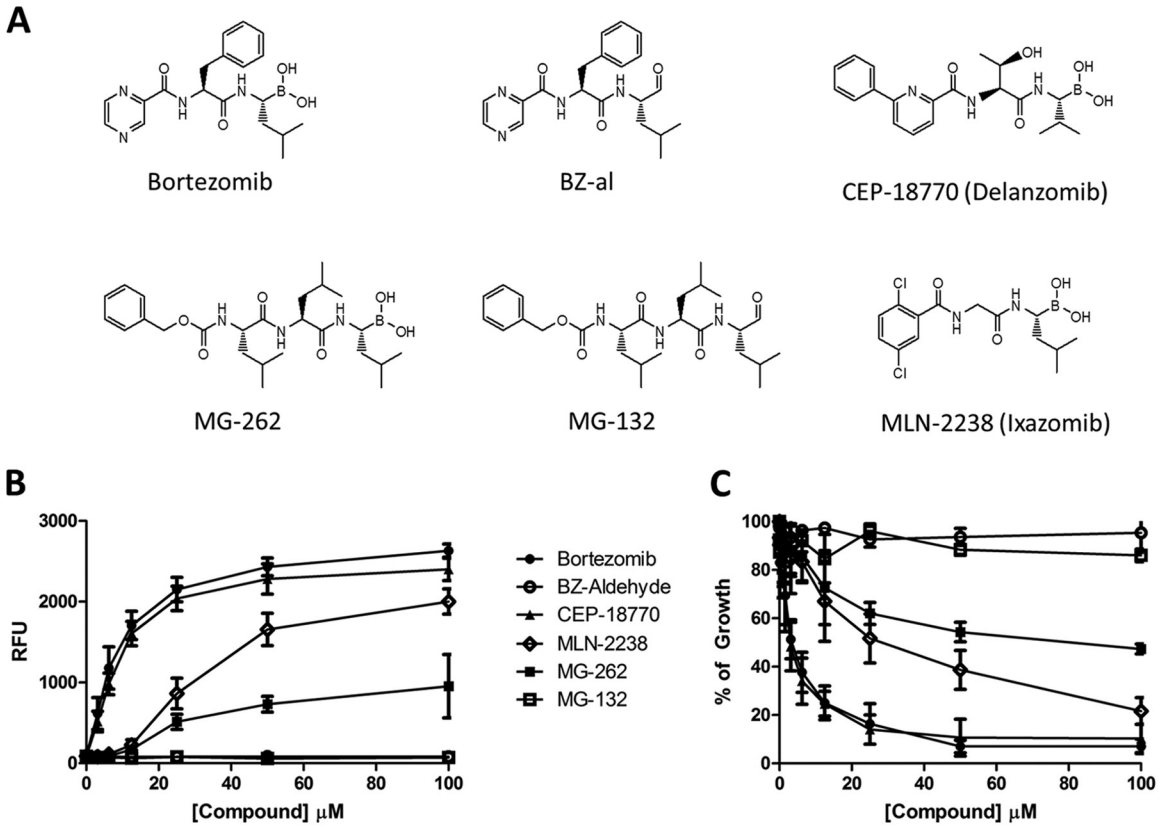

FIG 8 Correlation between ClpP1P2-dependent proteolytic activity and growth inhibition potencies of structural derivatives of BZ. (A) Structures of BZ and derivatives. (B) Inhibition of ClpP1P2 proteolytic activity. *M. smegmatis* p38-mRFP-SsrA was used as the reporter strain. (C) Inhibition of WT *M. smegmatis* growth. Responses to compounds at concentrations of up to 100 μM were assessed. Shown is the average of at three independent experiments with error bars representing the standard deviation. The same experiments were carried out with *M. bovis* p38-mRFP-SsrA (for RFU) and WT *M. bovis* (for growth inhibition), resulting in the same pattern observed with *M. smegmatis*. BZ and CEP-18770 showed a large RFU level increase and the strongest growth inhibition, MLN-2238 and MG-262 showed medium strength, and BZ-al and MG-132 showed no response in either assay (data not shown).

bacilli *M. bovis* BCG and *M. tuberculosis* H37Rv, consistent with previous ClpP1P2 genetic depletion data. Six additional lines of evidence suggest that BZ indeed exerts its antibacterial activity via inhibition of the caseinolytic protease. (i) Modulation of the intracellular ClpP1P2 level via genetic under- and overexpression resulted in BZ hyper- and hyposensitivity of the bacteria. (ii) The drug potentiated the effect of aminoglycosides, phenocopying ClpP1P2 hypomorphs. (iii) BZ exposure resulted in accumulation of the ClpP1P2-specific substrate WhiB1. (iv) Whole-cell growth inhibition potencies of BZ derivatives correlated with inhibition potencies against ClpP1P2 activity. (v) Replacement of the "anti-protease" boronic acid warhead of BZ with an aldehyde resulted in an inactive compound in both the ClpP1P2 activity and growth inhibition assays. (vi) Molecular modeling of BZ and its boronic acid derivatives showed that they can be covalently attached to ClpP1P2 catalytic sites.

This work has several implications. First, it demonstrates the feasibility of target mechanism-based whole-cell screening methods as a new approach to antimycobacterial drug discovery. Since the drug discovery community has returned to rather inefficient black-box whole-cell strategies, new avenues that reconnect antibacterial discovery with modern genome biology are urgently needed (5). Target mechanism-based screening methods might be a useful complement for other ongoing activities employing path-

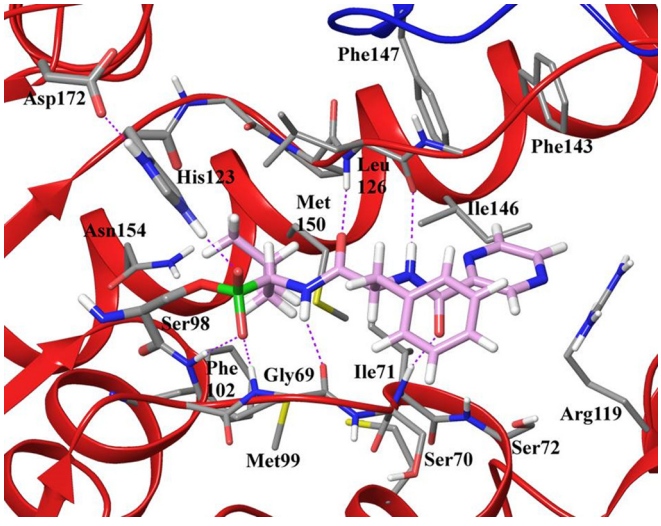

FIG 9 Modeling of BZ into one of the seven ClpP1 catalytic sites of ClpP1P2. ClpP1 is shown as a red ribbon, and ClpP2 is shown as a blue ribbon. The binding site residues are shown with grey carbon in thin-stick form, while the catalytic triad of Ser98, His123, and Asp172 is shown in thick-stick form. BZ is shown with plum-colored carbon in thick-stick form. Hydrogen bonds between BZ and ClpP1P2 are shown as purple dashed lines. The boronic acid of BZ is covalently attached to the catalytic serine. Boron is green.

way screening methods with hypersensitized bacterial strains and pathway stress-specific promoters.

Second, we provide chemical validation of mycobacterial ClpP1P2 as a target for TB therapy. Using BZ, we show for the first time that a small-molecule inhibitor of ClpP1P2 can indeed inhibit growth and kill mycobacteria, demonstrating pharmacologically the vulnerability and microbicidal potential of ClpP1P2. It should be noted that lactone derivatives with antimycobacterial properties have been proposed to act through inhibition of the caseinolytic protease (lactones 4 and 7 in references 39 and 40). However, these compounds displayed a dramatic disconnect between biochemical (mM) and growth-inhibitory (μM) potencies, suggesting that the antibacterial activity of these compounds is off target, i.e., unrelated to the weak, biochemically observed anti-ClpP1P2 activity. Indeed, lactones were not positive in either our ClpP1P2 activity reporter strain or our ClpP1P2-underexpressing, hypersensitized strain (data not shown). It is interesting that several molecules, including acyldepsipeptides and cyclomarin, have been identified that appear to increase the promiscuity of the caseinolytic protease complex and thus allow unspecific degradation of proteins (41, 42). Furthermore, lassomycin was recently found to stimulate the ATPase activity of a regulatory subunit of the caseinolytic protease while uncoupling it from the proteolytic activity of the complex (43). Our discovery of the first ClpP1P2-targeting whole-cell-active inhibitor adds to the growing list of caseinolytic protease modulators and shows that this proteolytic degradation machine represents an attractive multimechanism, multitarget complex for chemotherapeutic intervention.

Third, we identified BZ, a human-proteasome-targeting anticancer drug in clinical use, as a new lead compound for TB. Interestingly, mycobacteria are among the few prokaryotes that possess a proteasome like that of mammals (44). Whereas this function is dispensable (nonessential) in *M. smegmatis* (45), the proteasome is essential in the tubercle bacillus (46–48). This might explain why we see stronger antibacterial potency of BZ against *M. bovis* BCG and *M. tuberculosis* H37Rv than against *M. smegmatis*: in the tubercle bacillus, BZ might inhibit both ClpP1P2 and the tubercle bacillus' proteasome. Indeed, BZ has been used in biochemical studies of the *M. tuberculosis* proteasome (49–51).

BZ is given intravenously and has a short half-life (35, 36). In addition to an unfavorable route of administration and poor pharmacokinetics, high cost and significant adverse effects, including peripheral neuropathy, neutropenia, and cytopenia (35, 36) obviously limit its direct use for TB. Second-generation proteasome inhibitors, including orally bioavailable prodrugs, are in development. It is worth mentioning that we tested one of the boronic acid ester prodrugs, MNL-9708 (52, 53), and found the compound to be active in both our ClpP1P2 reporter and growth inhibition assays (data not shown). This suggests that introduction of oral bioavailability in a TB lead optimization program might be achievable. Considering the availability of *in vitro* assays for potency determination, the tools required for introducing selectivity, and the structural differences between the human proteasome and the mycobacterial caseinolytic protease (27, 33, 54, 55), BZ optimization appears to be an attractive opportunity.

In conclusion, our work demonstrates the feasibility of target mechanism-based whole-cell screening methods for antimycobacterial drug discovery, provides chemical validation of ClpP1P2 as a target for TB therapy, and identifies BZ as a new lead compound.

MATERIALS AND METHODS

Bacterial strains, culture medium, and chemicals. *M. smegmatis* mc^{2}155 (ATCC 700084), *M. bovis* BCG (ATCC 35734), and *M. tuberculosis* H37Rv (ATCC 27294) WT strains and derived GFP and mRFP reporter strains were maintained in Middlebrook 7H9 medium (Difco) supplemented with 0.5% (vol/vol) glycerol, 0.05% (vol/vol) Tween 80, and 10% (vol/vol) Middlebrook albumin-dextrose-catalase (Difco). When appropriate, hygromycin B (Roche) and ATc (Acros Organic) were added. Enumeration of bacteria was performed by plating on Middlebrook 7H10 (Difco) agar plates containing 0.5% (vol/vol) glycerol and 10% (vol/vol) Middlebrook oleic acid-albumin-dextrose-catalase (Difco). Antibiotics were purchased from Sigma-Aldrich. Stock solutions of the compounds were prepared in 90% dimethyl sulfoxide (DMSO). The Experimental Therapeutic Center's small-molecule compound library was collected from various commercial providers and consists of 13 sublibraries.

GFP and mRFP plasmid constructs and reporter strains. Plasmid pTet-GFP comprises the WT allele of the GFP gene cloned downstream of tetracycline-inducible pTet. GFP was amplified from GFPmut3 WT DNA via PCR and subsequently recombined into the pTet vector by gateway recombination (Clontech) as previously described (56). The GFP-SsrA fusion was generated via amplification from the same template with primers GGGGACAAGTTTGTACAAAAAAGCAGGCTGAAGGAGATATACATATGGCTAGCAAAGGAGAAGAAC and GGGGACCACTTTGTACAAGAAAGCTGGGTCGGCAGCGAGAGCGTAGTCG and cloned into the same vectors to generate pTet-GFP-SsrA. Plasmids pTET-GFP and pTet-GFP-SsrA were electroporated separately into WT *M. smegmatis* to generate strains Smeg-pTet-GFP and Smeg-pTet-GFP-SsrA, respectively. Plasmid pGMEH-p38-mRFP carries the gene for mRFP cloned downstream of the p38 strong mycobacterial promoter (57). pGMEH-p38-mRFP-SsrAec carries the same construct including the *Escherichia coli* SsrA tag fused to the mRFP gene. Both plasmids were obtained from Addgene (no. 27058 and 27059) and electroporated into WT *M. smegmatis* to generate Smeg-p38-mRFP and Smeg-p38-mRFP-SsrA, respectively.

pTet-GFP-SsrA assay optimization and high-throughput primary screening. Smeg-pTet-GFP and Smeg-pTet-GFP-SsrA precultures were harvested at mid-log phase and diluted to an OD_{600} of 0.2 in complete 7H9 medium. ATc was added when appropriate, and the bacterial suspension was distributed into the wells (30 μl/well) of a flat-bottom, dark, medium-binding 384-well plate (Greiner Bio-One) and incubated at 37°C for 3 h. Fluorescence signals (in relative fluorescence units [RFU]) were measured with a Synergy H1 microplate reader (BioTek) (excitation wavelength, 485 nm; emission wavelength, 520 nm) with a 90-s shaking step prior to reading. OD normalization between strains was verified by bacterial enumeration as mentioned above. DMSO tolerance was assessed by growing the strains in 7H9 medium with increasing concentrations of DMSO and measuring the effect on fluorescence levels, as well as plating the cells and determining CFU counts. Following optimization of the primary screening assay, a high-throughput format was validated by the same procedure. Prior to screening of the complete 503,879-compound library, the PHARMAKON 1600 library (1,600 compounds) was used in a validation run to assess the performance indicators of the assay under high-throughput conditions. The Z′ factor, a measure of assay performance, was calculated as follows: $Z' = 1 - [(3\sigma_{c+} + 3\sigma_{c-})/(\mu_{c+} - \mu_{c-})]$, where μ_{c+} and μ_{c-} are the mean positive- and negative-control signals and σ_{c+} and σ_{c-} are the respective standard deviations. Screening results were accepted only if the Z′ factor was >0.5. We used topotecan (Sigma-Aldrich) as a positive control for inhibitor screening. Each compound was screened in duplicate at a final concentration of 10 μM. GFP signals were measured with a Safire II microplate reader (Tecan) by using the same parameters as described above. Hits were defined as compounds that induced a GFP signal response higher than a cutoff value defined by the mean plus twice the standard deviation and were submitted to a retest

in an identical assay. Autofluorescence of retest-positive hits was measured by dispensing each compound at 10 μM (in 90% DMSO) into the wells of a 384-well plate and measuring the fluorescence signal by using the same signal acquisition parameters as for the primary screening. Autofluorescent compounds were filtered out. We next evaluated the GFP dose-response profiles of all of the inhibitor hits and determined their respective GFP IC_{50}s. Briefly, all of the selected hits were tested in a 3-fold serial-dilution GFP assay at a maximum concentration of 100 μM in a 96-well plate format of the GFP assay with an M200 PRO plate reader (Tecan).

Constitutive p38-mRFP secondary assay. All 89 selected hits from the primary screening results were reordered and subjected to secondary screening assays from fresh-powder stocks (90% DMSO) with *M. smegmatis* carrying a constitutive mRFP reporter system. We first proceeded with optimization and validation of the secondary assay as described above. We then proceeded to rescreen selected hits with Smeg-p38-mRFP-SsrA. Preculture samples were harvested at mid-log phase, diluted to an OD_{600} of 0.2 in complete 7H9 medium and dispensed into 96-well plates (200 μl/well) in the presence of compounds. Smeg-p38-mRFP-SsrA alone was used as a negative control, and Smeg-p38-mRFP was used as a positive control. Fluorescence signal acquisition was carried out with an M200 PRO plate reader (Tecan) after 3 h of incubation. Red fluorescence was acquired with excitation and emission wavelengths of 587 and 630 nm, respectively.

Turbidity-based growth inhibition assay. An inhibition assay of selected hits was performed to assess their inhibition potency. *M. smegmatis*, *M. bovis* BCG, and *M. tuberculosis* H37Rv precultures were harvested at mid-log phase and diluted to an OD_{600} of 0.05 in complete 7H9 medium. Bacterial suspensions were then dispensed into the wells of 96-well plates (200 μl/well) with the indicated compound concentration and incubated for 24 h (*M. smegmatis*) or 5 days (BCG and H37Rv) at 37°C with shaking (100 rpm). Cells were manually resuspended, and OD_{600} was measured on an M200 PRO plate reader (Tecan). Ciprofloxacin was used as a positive control.

Aminoglycoside potentiation assay. WT *M. smegmatis* (inoculum OD_{600} of 0.01 in 1 ml of 7H9) was treated with subinhibitory concentrations of BZ (1.5 μM) and other drugs as shown in Fig. 6, either independently or in combination where indicated. After 24 h, growth was assessed via OD_{600} measurement and growth inhibition was determined.

pTet-GFP-WhiB1 assay. *M. smegmatis* pTet-GFP-WhiB1 preculture was harvested at mid-log phase, diluted to an OD_{600} of 0.2 in complete 7H9 medium, and dispensed into the wells of 96-well plates (200 μl/well) in the presence of ATc and BZ were indicated. *M. smegmatis* pTet-GFP was used as a control and assessed under similar conditions. Cells were incubated for 6 h and manually resuspended, and fluorescence signals were acquired as described above.

Protein purification and immunoblotting. Total protein lysates were prepared from equivalent cell numbers by bead beating. After probing with primary antibody, visualization was performed with horseradish peroxidase-conjugated secondary antibodies (Invitrogen) and detection was performed with Western Lighting Plus-ECL (PerkinElmer) according the manufacturer's protocol. In all cases, blots were probed with an anti-RpoB monoclonal antibody (Abcam) to ensure equivalent loading of samples.

ClpP1P2 under- and overexpression and GFP-WhiB1 strains. The engineering of *M. smegmatis* pTet(chromosome)-ClpP1P2, in which the native promoter of ClpP1P2 has been replaced with a tetracycline-inducible promoter, and of *M. smegmatis* carrying an episomal copy of ClpP1P2 under the control of a tetracycline-inducible promoter (*M. smegmatis* pTet-ClpP1P2), in which ClpP1P2 overexpression can be induced by ATc, has been previously described (26). *M. smegmatis* pTet-GFP-WhiB1 carrying an episomal copy of the gene for WhiB1 fused to the gene for GFP and placed under the control of the pTet promoter has been described elsewhere (25).

Molecular modeling. The *M. tuberculosis* ClpP1P2 X-ray structure of 4U0G was downloaded from the Protein Data Bank (55). Addition of hydrogen atoms, setting of protonation and tautomer states, and hydrogen bond network optimization were done with the Protein Preparation Wizard in Maestro (Schrodinger Suite version 2014-2, 2014; Schrödinger, LLC, New York, NY). ClpP1P2 has 14 catalytic sites. The catalytic triad of the seven ClpP1 sites consists of residues Ser98, His123, and Asp172, and that of the seven ClpP2 sites consists of residues Ser110, His135, and Asp186. The conformation of BZ from the yeast 20S proteasome X-ray structure 4FWD (33) was manually positioned in the ClpP1P2 catalytic sites in an orientation that allowed hydrogen bonding between both amide NH donors and both amide carbonyls of BZ and protein backbone residues. These are Gly69, Ile71, and Leu126 of the ClpP1 sites and Gly81, Phe83, and Ser138 of the ClpP2 sites. The boronic acid was covalently attached to the catalytic serine, Ser98 in ClpP1 and Ser110 in ClpP2. One oxygen of the boronic acid group occupied the oxyanion hole hydrogen bonding with the backbone NH of Gly69 and Met99 in ClpP1 and Gly81 and Ala111 in ClpP2. The other boronic acid oxygen formed a salt bridge with the catalytic histidine, His123 of ClpP1 and His135 of ClpP2. This complex was minimized by using the OPLS2005 force field, the generalized born surface area salvation model, 500 steps of the Polak-Ribière conjugate gradient method, and the MacroModel default settings (Schrodinger Suite version 2014-2, 2014; Schrödinger, LLC, New York, NY). All residues more than 12 Å from BZ were constrained during minimization. Delanzomib, MG-262, and ixazomib were also modeled into ClpP1P2 by using the conformation of BZ as a template, and the complexes were minimized.

ACKNOWLEDGMENTS

We thank Shan Ho Tan of the Experimental Therapeutics Center for his help with information technology-related matters and the anonymous reviewers for their expert suggestions. We are grateful to D. Schnappinger and S. Ehrt for sharing the RFP and RFP-SsrA plasmids via Addgene.

This study was funded by a grant from the Singapore Ministry of Health, National Medical Research Council, (NMRC/CBRG/0022/2012) to T.D. G.J.Y.N. received a scholarship from the Singapore-MIT Alliance on Research and Technology, SMART. We acknowledge support by the Yong Loo Lin School of Medicine BSL-3 Core Facility and the Singapore Ministry of Health, National Medical Research Council, center grant MINE, Research Core no. 4 (NMRC/CG/013/2013) to T.D.

W.M., R.R., E.R., and T.D. conceived the project and designed the strategy. R.R. an E.R. developed the *M. smegmatis* strains carrying the pTet-GFP-SsrA and pTet-GFP-WhiB1 reporter systems, as well as *M. smegmatis* ClpP1P2-over- and -underexpressing strains. W.M. and G.J.Y.N. developed the *M. smegmatis* and *M. bovis* BCG strains carrying p38-mRFP-SsrA reporter systems. W.M., G.J.Y.N., and J.L.L developed and carried out all of the non-HTS assays. W.M., A.Y., J.F., U.L., J.L., A.T., H.F., and F.H. supervised, conducted, and collected the HTS assay data. B.C.S.C. and M.J.Y.A. synthesized the BZ analogue BZ-al. A.P. did the molecular modeling. W.M. and T.D. executed the project, analyzed the data, and wrote the manuscript.

We have no competing or other interests that might be perceived to influence the results and discussion reported in this paper.

REFERENCES

1. **World Health Organization**. 2013. Global tuberculosis report 2013. World Health Organization, Geneva, Switzerland. http://apps.who.int/iris/bitstream/10665/91355/1/9789241564656_eng.pdf.
2. **Koul A, Arnoult E, Lounis N, Guillemont J, Andries K**. 2011. The challenge of new drug discovery for tuberculosis. Nature **469:**483–490. http://dx.doi.org/10.1038/nature09657.
3. **Gwynn MN, Portnoy A, Rittenhouse SF, Payne DJ**. 2010. Challenges of antibacterial discovery revisited. Ann N Y Acad Sci **1213:**5–19. http://dx.doi.org/10.1111/j.1749-6632.2010.05828.x.
4. **Payne DJ, Gwynn MN, Holmes DJ, Pompliano DL**. 2007. Drugs for bad bugs: confronting the challenges of antibacterial discovery. Nat Rev Drug Discov **6:**29–40. http://dx.doi.org/10.1038/nrd2201.

5. **Brötz-Oesterhelt H, Sass P.** 2010. Postgenomic strategies in antibacterial drug discovery. Future Microbiol **5:**1553–1579. http://dx.doi.org/10.2217/fmb.10.119.
6. **Pethe K, Sequeira PC, Agarwalla S, Rhee K, Kuhen K, Phong WY, Patel V, Beer D, Walker JR, Duraiswamy J, Jiricek J, Keller TH, Chatterjee A, Tan MP, Ujjini M, Rao SP, Camacho L, Bifani P, Mak PA, Ma I, Barnes SW, Chen Z, Plouffe D, Thayalan P, Ng SH, Au M, Lee BH, Tan BH, Ravindran S, Nanjundappa M, Lin X, Goh A, Lakshminarayana SB, Shoen C, Cynamon M, Kreiswirth B, Dartois V, Peters EC, Glynne R, Brenner S, Dick T.** 2010. A chemical genetic screen in Mycobacterium tuberculosis identifies carbon-source-dependent growth inhibitors devoid of in vivo efficacy. Nat Commun **1:**57. http://dx.doi.org/10.1038/ncomms1060.
7. **Wei JR, Krishnamoorthy V, Murphy K, Kim JH, Schnappinger D, Alber T, Sassetti CM, Rhee KY, Rubin EJ.** 2011. Depletion of antibiotic targets has widely varying effects on growth. Proc Natl Acad Sci U S A **108:**4176–4181. http://dx.doi.org/10.1073/pnas.1018301108.
8. **Dick T, Young D.** 2011. How antibacterials really work: impact on drug discovery. Future Microbiol **6:**603–604. http://dx.doi.org/10.2217/fmb.11.26.
9. **Barry CE III, Boshoff HI, Dartois V, Dick T, Ehrt S, Flynn J, Schnappinger D, Wilkinson RJ, Young D.** 2009. The spectrum of latent tuberculosis: rethinking the biology and intervention strategies. Nat Rev Microbiol **7:**845–855. http://dx.doi.org/10.1038/nrmicro2236.
10. **Brötz-Oesterhelt H, Sass P.** 2010. Postgenomic strategies in antibacterial drug discovery. Future Microbiol **5:**1553–1579. http://dx.doi.org/10.2217/fmb.10.119.
11. **Wang J, Soisson SM, Young K, Shoop W, Kodali S, Galgoci A, Painter R, Parthasarathy G, Tang YS, Cummings R, Ha S, Dorso K, Motyl M, Jayasuriya H, Ondeyka J, Herath K, Zhang C, Hernandez L, Allocco J, Basilio A, Tormo JR, Genilloud O, Vicente F, Pelaez F, Colwell L, Lee SH, Michael B, Felcetto T, Gill C, Silver LL, Hermes JD, Bartizal K, Barrett J, Schmatz D, Becker JW, Cully D, Singh SB.** 2006. Platensimycin is a selective FabF inhibitor with potent antibiotic properties. Nature **441:**358–361. http://dx.doi.org/10.1038/nature04784.
12. **Brötz-Oesterhelt H, Sass P.** 2014. Bacterial caseinolytic proteases as novel targets for antibacterial treatment. Int J Med Microbiol **304:**23–30. http://dx.doi.org/10.1016/j.ijmm.2013.09.001.
13. **Abrahams GL, Kumar A, Savvi S, Hung AW, Wen S, Abell C, Barry CE III, Sherman DR, Boshoff HI, Mizrahi V.** 2012. Pathway-selective sensitization of Mycobacterium tuberculosis for target-based whole-cell screening. Chem Biol **19:**844–854. http://dx.doi.org/10.1016/j.chembiol.2012.05.020.
14. **Ferrand S, Tao J, Shen X, McGuire D, Schmid A, Glickman JF, Schopfer U.** 2011. Screening for mevalonate biosynthetic pathway inhibitors using sensitized bacterial strains. J Biomol Screen **16:**637–646. http://dx.doi.org/10.1177/1087057111403927.
15. **Forsyth RA, Haselbeck RJ, Ohlsen KL, Yamamoto RT, Xu H, Trawick JD, Wall D, Wang L, Brown-Driver V, Froelich JM, C, KG, King P, McCarthy M, Malone C, Misiner B, Robbins D, Tan ZY, Zhu Zy, ZY, Carr G, Mosca DA, Zamudio C, Foulkes JG, Zyskind JW.** 2002. A genome-wide strategy for the identification of essential genes in Staphylococcus aureus. Mol Microbiol **43:**1387–1400. http://dx.doi.org/10.1046/j.1365-2958.2002.02832.x.
16. **Wang J, Kodali S, Lee SH, Galgoci A, Painter R, Dorso K, Racine F, Motyl M, Hernandez L, Tinney E, Colletti SL, Herath K, Cummings R, Salazar O, González I, Basilio A, Vicente F, Genilloud O, Pelaez F, Jayasuriya H, Young K, Cully DF, Singh SB.** 2007. Discovery of platencin, a dual FabF and FabH inhibitor with in vivo antibiotic properties. Proc Natl Acad Sci U S A **104:**7612–7616. http://dx.doi.org/10.1073/pnas.0700746104.
17. **Wang H, Gill CJ, Lee SH, Mann P, Zuck P, Meredith TC, Murgolo N, She X, Kales S, Liang L, Liu J, Wu J, Santa Maria J, Su J, Pan J, Hailey J, Mcguinness D, Tan CM, Flattery A, Walker S, Black T, Roemer T.** 2013. Discovery of wall teichoic acid inhibitors as potential anti-MRSA beta-lactam combination agents. Chem Biol **20:**272–284. http://dx.doi.org/10.1016/j.chembiol.2012.11.013.
18. **Nisa S, Blokpoel MC, Robertson BD, Tyndall JD, Lun S, Bishai WR, O'Toole R.** 2010. Targeting the chromosome partitioning protein ParA in tuberculosis drug discovery. J Antimicrob Chemother **65:**2347–2358. http://dx.doi.org/10.1093/jac/dkq311.
19. **Park SW, Casalena DE, Wilson DJ, Dai R, Nag PP, Liu F, Boyce JP, Bittker JA, Schreiber SL, Finzel BC, Schnappinger D, Aldrich CC.** 2015. Target-based identification of whole-cell active inhibitors of biotin biosynthesis in Mycobacterium tuberculosis. Chem Biol **22:**76–86. http://dx.doi.org/10.1016/j.chembiol.2014.11.012.
20. **Fischer HP, Brunner NA, Wieland B, Paquette J, Macko L, Ziegelbauer K, Freiberg C.** 2004. Identification of antibiotic stress-inducible promoters: a systematic approach to novel pathway-specific reporter assays for antibacterial drug discovery. Genome Res **14:**90–98. http://dx.doi.org/10.1101/gr.1275704.
21. **Bogatcheva E, Hanrahan C, Chen P, Gearhart J, Sacksteder K, Einck L, Nacy C, Protopopova M.** 2010. Discovery of dipiperidines as new antitubercular agents. Bioorg Med Chem Lett **20:**201–205. http://dx.doi.org/10.1016/j.bmcl.2009.10.135.
22. **Wilson R, Kumar P, Parashar V, Vilchèze C, Veyron-Churlet R, Freundlich JS, Barnes SW, Walker JR, Szymonifka MJ, Marchiano E, Shenai S, Colangeli R, Jacobs WR, Jr., Neiditch MB, Kremer L, Alland D.** 2013. Antituberculosis thiophenes define a requirement for Pks13 in mycolic acid biosynthesis. Nat Chem Biol **9:**499–506. http://dx.doi.org/10.1038/nchembio.1277.
23. **Frees D, Andersen JH, Hemmingsen L, Koskenniemi K, Baek KT, Muhammed MK, Gudeta DD, Nyman TA, Sukura A, Varmanen P, Savijoki K.** 2012. New insights into Staphylococcus aureus stress tolerance and virulence regulation from an analysis of the role of the ClpP protease in the strains Newman, Col, and SA564. J Proteome Res **11:**95–108. http://dx.doi.org/10.1021/pr200956s.
24. **Frees D, Savijoki K, Varmanen P, Ingmer H.** 2007. Clp ATPases and ClpP proteolytic complexes regulate vital biological processes in low GC, Gram-positive bacteria. Mol Microbiol **63:**1285–1295. http://dx.doi.org/10.1111/j.1365-2958.2007.05598.x.
25. **Raju RM, Jedrychowski MP, Wei J, Pinkham JT, Park AS, O'Brien K, Rehren G, Schnappinger D, Gygi SP, Rubin EJ.** 2014. Post-translational regulation via Clp protease is critical for survival of Mycobacterium tuberculosis. PLoS Pathog **10:**e1003994. http://dx.doi.org/10.1371/journal.ppat.1003994.
26. **Raju RM, Unnikrishnan M, Rubin DH, Krishnamoorthy V, Kandror O, Akopian TN, Goldberg AL, Rubin EJ.** 2012. Mycobacterium tuberculosis ClpP1 and ClpP2 function together in protein degradation and are required for viability in vitro and during infection. PLoS Pathog **8:**e1002511. http://dx.doi.org/10.1371/journal.ppat.1002511.
27. **Akopian T, Kandror O, Raju RM, Unnikrishnan M, Rubin EJ, Goldberg AL.** 2012. The active ClpP protease from M. tuberculosis is a complex composed of a heptameric ClpP1 and a ClpP2 ring. EMBO J **31:**1529–1541. http://dx.doi.org/10.1038/emboj.2012.5.
28. **Keiler KC.** 2008. Biology of trans-translation. Annu Rev Microbiol **62:**133–151. http://dx.doi.org/10.1146/annurev.micro.62.081307.162948.
29. **Chen D, Frezza M, Schmitt S, Kanwar J, Dou QP.** 2011. Bortezomib as the first proteasome inhibitor anticancer drug: current status and future perspectives. Curr Cancer Drug Targets **11:**239–253. http://dx.doi.org/10.2174/156800911794519752.
30. **Kane RC, Bross PF, Farrell AT, Pazdur R.** 2003. Velcade: U.S. FDA approval for the treatment of multiple myeloma progressing on prior therapy. Oncologist **8:**508–513. http://dx.doi.org/10.1634/theoncologist.8-6-508.
31. **Kane RC, Dagher R, Farrell A, Ko CW, Sridhara R, Justice R, Pazdur R.** 2007. Bortezomib for the treatment of mantle cell lymphoma. Clin Cancer Res **13:**5291–5294. http://dx.doi.org/10.1158/1078-0432.CCR-07-0871.
32. **Bonvini P, Zorzi E, Basso G, Rosolen A.** 2007. Bortezomib-mediated 26S proteasome inhibition causes cell-cycle arrest and induces apoptosis in CD-30$^+$ anaplastic large cell lymphoma. Leukemia **21:**838–842. http://dx.doi.org/10.1038/sj.leu.2404528.
33. **Groll M, Berkers CR, Ploegh HL, Ovaa H.** 2006. Crystal structure of the boronic acid-based proteasome inhibitor bortezomib in complex with the yeast 20S proteasome. Structure **14:**451–456. http://dx.doi.org/10.1016/j.str.2005.11.019.
34. **Bergmann ED, Sicher S.** 1952. Mode of action of chloramphenicol. Nature **170:**931–932. http://dx.doi.org/10.1038/170931a0.
35. **Kisselev AF, van der Linden WA, Overkleeft HS.** 2012. Proteasome inhibitors: an expanding army attacking a unique target. Chem Biol **19:**99–115. http://dx.doi.org/10.1016/j.chembiol.2012.01.003.
36. **Kisselev AF, Goldberg AL.** 2001. Proteasome inhibitors: from research tools to drug candidates. Chem Biol **8:**739–758. http://dx.doi.org/10.1016/S1074-5521(01)00056-4.
37. **Adams J, Behnke M, Chen S, Cruickshank AA, Dick LR, Grenier L, Klunder JM, Ma YT, Plamondon L, Stein RL.** 1998. Potent and selective

inhibitors of the proteasome: dipeptidyl boronic acids. Bioorg Med Chem Lett **8:**333–338. http://dx.doi.org/10.1016/S0960-894X(98)00029-8.
38. **Adams J, Palombella VJ, Sausville EA, Johnson J, Destree A, Lazarus DD, Maas J, Pien CS, Prakash S, Elliott PJ.** 1999. Proteasome inhibitors: a novel class of potent and effective antitumor agents. Cancer Res **59:** 2615–2622.
39. **Compton CL, Schmitz KR, Sauer RT, Sello JK.** 2013. Antibacterial activity of and resistance to small molecule inhibitors of the ClpP peptidase. ACS Chem Biol **8:**2669–2677. http://dx.doi.org/10.1021/cb400577b.
40. **Gersch M, Gut F, Korotkov VS, Lehmann J, Böttcher T, Rusch M, Hedberg C, Waldmann H, Klebe G, Sieber SA.** 2013. The mechanism of caseinolytic protease (ClpP) inhibition. Angew Chem Int Ed Engl **52:** 3009–3014. http://dx.doi.org/10.1002/anie.201204690.
41. **Kirstein J, Hoffmann A, Lilie H, Schmidt R, Rübsamen-Waigmann H, Brötz-Oesterhelt H, Mogk A, Turgay K.** 2009. The antibiotic ADEP reprogrammes ClpP, switching it from a regulated to an uncontrolled protease. EMBO Mol Med **1:**37–49. http://dx.doi.org/10.1002/emmm.200900002.
42. **Schmitt EK, Riwanto M, Sambandamurthy V, Roggo S, Miault C, Zwingelstein C, Krastel P, Noble C, Beer D, Rao SP, Au M, Niyomrattanakit P, Lim V, Zheng J, Jeffery D, Pethe K, Camacho LR.** 2011. The natural product cyclomarin kills Mycobacterium tuberculosis by targeting the ClpC1 subunit of the caseinolytic protease. Angew Chem Int Ed Engl **50:**5889–5891. http://dx.doi.org/10.1002/anie.201101740.
43. **Gavrish E, Sit CS, Cao S, Kandror O, Spoering A, Peoples A, Ling L, Fetterman A, Hughes D, Bissell A, Torrey H, Akopian T, Mueller A, Epstein S, Goldberg A, Clardy J, Lewis K.** 2014. Lassomycin, a ribosomally synthesized cyclic peptide, kills Mycobacterium tuberculosis by targeting the ATP-dependent protease ClpC1P1P2. Chem Biol **21:** 509–518. http://dx.doi.org/10.1016/j.chembiol.2014.01.014.
44. **Darwin KH, Ehrt S, Gutierrez-Ramos JC, Weich N, Nathan CF.** 2003. The proteasome of Mycobacterium tuberculosis is required for resistance to nitric oxide. Science **302:**1963–1966. http://dx.doi.org/10.1126/science.1091176.
45. **Knipfer N, Shrader TE.** 1997. Inactivation of the 20S proteasome in Mycobacterium smegmatis. Mol Microbiol **25:**375–383. http://dx.doi.org/10.1046/j.1365-2958.1997.4721837.x.
46. **Sassetti CM, Boyd DH, Rubin EJ.** 2003. Genes required for mycobacterial growth defined by high density mutagenesis. Mol Microbiol **48:**77–84. http://dx.doi.org/10.1046/j.1365-2958.2003.03425.x.
47. **Sassetti CM, Rubin EJ.** 2003. Genetic requirements for mycobacterial survival during infection. Proc Natl Acad Sci U S A **100:**12989–12994. http://dx.doi.org/10.1073/pnas.2134250100.
48. **Griffin JE, Gawronski JD, Dejesus MA, Ioerger TR, Akerley BJ, Sassetti CM.** 2011. High-resolution phenotypic profiling defines genes essential for mycobacterial growth and cholesterol catabolism. PLoS Pathog **7:**e1002251. http://dx.doi.org/10.1371/journal.ppat.1002251.
49. **Lin G, Tsu C, Dick L, Zhou XK, Nathan C.** 2008. Distinct specificities of Mycobacterium tuberculosis and mammalian proteasomes for N-acetyl tripeptide substrates. J Biol Chem **283:**34423–34431. http://dx.doi.org/10.1074/jbc.M805324200.
50. **Hu G, Lin G, Wang M, Dick L, Xu RM, Nathan C, Li H.** 2006. Structure of the Mycobacterium tuberculosis proteasome and mechanism of inhibition by a peptidyl boronate. Mol Microbiol **59:**1417–1428. http://dx.doi.org/10.1111/j.1365-2958.2005.05036.x.
51. **Lin G, Li D, de Carvalho LP, Deng H, Tao H, Vogt G, Wu K, Schneider J, Chidawanyika T, Warren JD, Li H, Nathan C.** 2009. Inhibitors selective for mycobacterial versus human proteasomes. Nature **461:**621–626. http://dx.doi.org/10.1038/nature08357.
52. **Kupperman E, Lee EC, Cao Y, Bannerman B, Fitzgerald M, Berger A, Yu J, Yang Y, Hales P, Bruzzese F, Liu J, Blank J, Garcia K, Tsu C, Dick L, Fleming P, Yu L, Manfredi M, Rolfe M, Bolen J.** 2010. Evaluation of the proteasome inhibitor MLN9708 in preclinical models of human cancer. Cancer Res **70:**1970–1980. http://dx.doi.org/10.1158/0008-5472.CAN-09-2766.
53. **Chauhan D, Tian Z, Zhou B, Kuhn D, Orlowski R, Raje N, Richardson P, Anderson KC.** 2011. In vitro and in vivo selective antitumor activity of a novel orally bioavailable proteasome inhibitor MLN9708 against multiple myeloma cells. Clin Cancer Res **17:**5311–5321. http://dx.doi.org/10.1158/1078-0432.CCR-11-0476.
54. **Raju RM, Goldberg AL, Rubin EJ.** 2012. Bacterial proteolytic complexes as therapeutic targets. Nat Rev Drug Discov **11:**777–789. http://dx.doi.org/10.1038/nrd3846.
55. **Schmitz KR, Carney DW, Sello JK, Sauer RT.** 2014. Crystal structure of Mycobacterium tuberculosis ClpP1P2 suggests a model for peptidase activation by AAA^+ partner binding and substrate delivery. Proc Natl Acad Sci U S A **111:**E4587–E4595. http://dx.doi.org/10.1073/pnas.1417120111.
56. **Hartley JL, Temple GF, Brasch MA.** 2000. DNA cloning using in vitro site-specific recombination. Genome Res **10:**1788–1795. http://dx.doi.org/10.1101/gr.143000.
57. **Kim JH, Wei JR, Wallach JB, Robbins RS, Rubin EJ, Schnappinger D.** 2011. Protein inactivation in mycobacteria by controlled proteolysis and its application to deplete the beta subunit of RNA polymerase. Nucleic Acids Res **39:**2210–2220. http://dx.doi.org/10.1093/nar/gkq1149.